magnetochemistry

MDPI

Article

Calcium-Dependent Interaction Occurs between Slow Skeletal Myosin Binding Protein C and Calmodulin

Tzvia I. Springer [1,†], Christian W. Johns [2], Jana Cable [1], Brian Leei Lin [3], Sakthivel Sadayappan [4] and Natosha L. Finley [1,2,*]

1 Department of Microbiology, Miami University, Oxford, OH 45056, USA; tspringer@mcw.edu (T.I.S.); cablejm@miamioh.edu (J.C.)
2 Cell, Molecular, and Structural Biology Program, Miami University, Oxford, OH 45056, USA; johnscw@miamioh.edu
3 Department of Cardiology, Johns Hopkins University, Baltimore, MD 21205, USA; blin29@jhmi.edu
4 Department of Internal Medicine, Heart Branch of the Heart, Lung and Vascular Institute, University of Cincinnati College of Medicine, Cincinnati, OH 45267, USA; SADAYASL@ucmail.uc.edu
* Correspondence: finleynl@miamioh.edu; Tel.: +1-513-529-0950
† Present affiliation Department of Biophysics, Medical College of Wisconsin, 8701 W. Watertown Plank Road, Milwaukee, WI 2042, USA.

Received: 1 November 2017; Accepted: 15 December 2017; Published: 21 December 2017

Abstract: Myosin binding protein C (MyBP-C) is a multi-domain protein that participates in the regulation of muscle contraction through dynamic interactions with actin and myosin. Three primary isoforms of MyBP-C exist: cardiac (cMyBP-C), fast skeletal (fsMyBP-C), and slow skeletal (ssMyBP-C). The N-terminal region of cMyBP-C contains the M-motif, a three-helix bundle that binds Ca^{2+}-loaded calmodulin (CaM), but less is known about N-terminal ssMyBP-C and fsMyBP-C. Here, we characterized the conformation of a recombinant N-terminal fragment of ssMyBP-C (ssC1C2) using differential scanning fluorimetry, nuclear magnetic resonance, and molecular modeling. Our studies revealed that ssC1C2 has altered thermal stability in the presence and absence of CaM. We observed that site-specific interaction between CaM and the M-motif of ssC1C2 occurs in a Ca^{2+}-dependent manner. Molecular modeling supported that the M-motif of ssC1C2 likely adopts a three-helix bundle fold comparable to cMyBP-C. Our study provides evidence that ssMyBP-C has overlapping structural determinants, in common with the cardiac isoform, which are important in controlling protein–protein interactions. We shed light on the differential molecular regulation of contractility that exists between skeletal and cardiac muscle.

Keywords: calcium; calmodulin; molecular model; MyBP-C; NMR; protein

1. Introduction

Myosin binding protein C (MyBP-C) is a modular protein composed of immunoglobulin (Ig) domains and fibronectin type III (FN3) repeats. It is reported to span between thin and thick filaments [1] while participating in the regulation of actin–myosin association. The N-terminal domains of MyBP-C interact with actin [2–8], myosin S2 [9,10], and the regulatory light chains [11], while the C-terminal domains are tethered to titin [12] and the myosin rod [13–15]. There are three different isoforms of MyBP-C expressed in striated muscles: cardiac (cMyBP-C), fast skeletal (fsMyBP-C), and slow skeletal (ssMyBP-C). Primarily, fsMyBP-C expression is localized to fast skeletal muscle, whereas ssMyBP-C is expressed in both slow and fast skeletal muscle [16]. The expression of cMyBP-C is localized to the heart, where its role as a dynamic regulator of cardiac contractility is established. Mutations in the genes encoding for each MyBP-C isoforms are associated with the development diseases such as distal arthrogryposis and hypertrophic cardiomyopathy. Interestingly, expression

of mutant cMyBP-C appears to be associated with the progression of skeletal myopathies, but the molecular basis is poorly understood. Ablation of cMyBP-C leads to increased expression of fsMyBP-C in heart muscle, but its presence does not restore cardiac contractility in heart failure (HF) models [17]. While there seems to be a link between spatial and temporal expression of MyBP-C isoforms in normal and diseased muscles, the functional consequences of isoform switching remain unclear. Certainly, the fact that skeletal and cardiac MyBP-C preferentially interact with their isoform-specific variants of actin and myosin [18] suggests that each protein may be structurally and functionally distinct.

Although skeletal and cardiac MyBP-C isoforms have approximately 50–70% sequence homology at the amino acid level, there are global differences in protein architecture that potentially impact control of contractility. Unlike fsMyBP-C and ssMyBP-C, cMyBP-C has a cardiac specific N-terminal domain denoted C0 and an additional loop in the C5 domain [19,20]. The presence of unique phosphorylation sites in the M-motif of cMyBP-C influences the force and frequency of contraction in the heart. In addition to association with myosin S2, the M-motif of cMyBP-C exerts its regulatory effects through actin [3,21–24] and calcium-calmodulin (Ca^{2+}-CaM) interactions [25]. The Ca^{2+}-dependent CaM protein kinase (CaMK) covalently modifies S282, which in turn promotes phosphorylation by protein kinase A (PKA) or protein kinase C (PKC) at sites S273 and S302 [8,10]. PKA phosphorylation sites have been identified in ssMyBP-C [26], but phosphorylation in fsMyBP-C is largely uncharacterized. Considerably less is known about the role of phosphorylation in regulating contraction in fast and slow skeletal muscles. However, there is a critical link between Ca^{2+}-signaling and cardiac function that is mediated in part by the interaction of the M-motif with CaM.

CaM is composed of two globular lobes connected by a flexible tether. Each N- and C-terminal domain has two EF-hand motifs that coordinate Ca^{2+} in the presence of saturating intracellular Mg^{2+} concentrations. In response to ligating Ca^{2+}, the globular domains undergo conformational transitions that expose the hydrophobic pockets necessary for target recognition. CaM exhibits a great degree of conformational plasticity, facilitated by dynamic motion in the linker region. One mode of interaction involves the formation of an extended complex, whereby both lobes of CaM are held apart by binding to protein targets, as is observed in numerous biological systems [27,28]. Alternatively, the lobes of CaM can engage a target protein by collapsing around it in a fashion similar to the complex formed with CaM-dependent kinases [29]. Although there is no single canonical CaM-binding motif, protein targets involved in its interaction typically have hydrophobic and positively charged amino residues involved in CaM recognition. Lu et al. report that CaM mostly associates with the M-motif of cMyBP-C through the insertion of a tryptophan residue into the hydrophobic pockets of Ca^{2+}-loaded CaM. Moreover, basic amino acid residues mapping to the M-motif are conformationally perturbed in the presence of CaM, further supporting the idea that this region is involved in protein–protein association. Comparison of amino acid sequence alignments reveals that M-motif residues are highly conserved in MyBP-C, including the skeletal isoforms, but the structural and functional significance remain to be determined [30].

Based on previous animal model studies [17], skeletal and cardiac MyBP-C are proposed to have functionally disparate roles in regulating contractility, but the molecular and structural bases are unknown. In this study, we use biophysical techniques to structurally characterize slow skeletal MyBP-C (ssMyBP-C). The conformation and protein binding properties of an N-terminal recombinant fragment of ssMyBP-C (ssC1C2) were examined by differential scanning fluorimetry (DSF), nuclear magnetic resonance (NMR) spectroscopy, and molecular modeling. The conformation of ssC1C2 was modulated in the presence of Ca^{2+}-loaded CaM as evidenced by the detection of altered protein thermal stability. NMR binding experiments were performed to demonstrate that site-specific interactions between ssC1C2 and Ca^{2+}-CaM are mediated through hydrophobic surfaces. Using protein homology modeling, we examined the tertiary structure of the M-motif, a region of ssMyBP-C known to be of importance in protein binding. Our findings support that ssC1C2 associates with CaM in a Ca^{2+}-dependent manner through hydrophobic interaction mediated by the M-motif, which may have significance in the differential regulation of skeletal and cardiac muscle contractility.

2. Results

2.1. Analysis of Amino Acid Conservation Provides Clues about Regulatory Functions in MyBP-C Isoforms

Using the CLUSTAL Omega server, we aligned the primary sequences corresponding to the N-terminal fragments of MyBP-C [31]. Analyses of primary structure of amino acid sequences corresponding to the N-terminal domains of MyBP-C revealed that significant amino acid similarities exist between the skeletal and cardiac isoforms (~50%) (Figure 1). Most notably, the regions known to be involved in actin and myosin binding in cMyBP-C domains (C0C2) [2], exhibited the highest degree of amino acid conservation between the isoforms. Overlapping binding determinants for actin and myosin were located in the C1 domain for skeletal and cardiac isoforms, suggesting that ssC1C2 and fsC1C2 associates with cardiac filament proteins in manner similar to that observed for cMyBP-C. Similarly, many amino acid residues in the M-motif of cMyBP-C that are known to experience conformational perturbations in the presence of CaM [25] were also conserved in ssC1C2 and fsC1C2. While other studies report PKA and PKC sites in ssMyBP-C [32], the structural and functional roles of CaMK phosphorylation in skeletal MyBP-C remain to be determined. Using bioinformatics tools, we identified phosphorylation sites for CaMK located at specific regions in the C1 and C2, near the M-motif, of both ssC1C2 and fsC1C2 (Table S1). Interestingly, these predicted phosphorylation sites in ssMyBP-C and fsMyPB-C proteins are proximal to highly conserved actin, CaM, and myosin binding motifs in cMyBP-C. Taken together, these observations suggest that the skeletal proteins might have similar target recognition sites as compared to cMyBP-C and that post-translational modifications within these regions may modulate protein–protein interactions.

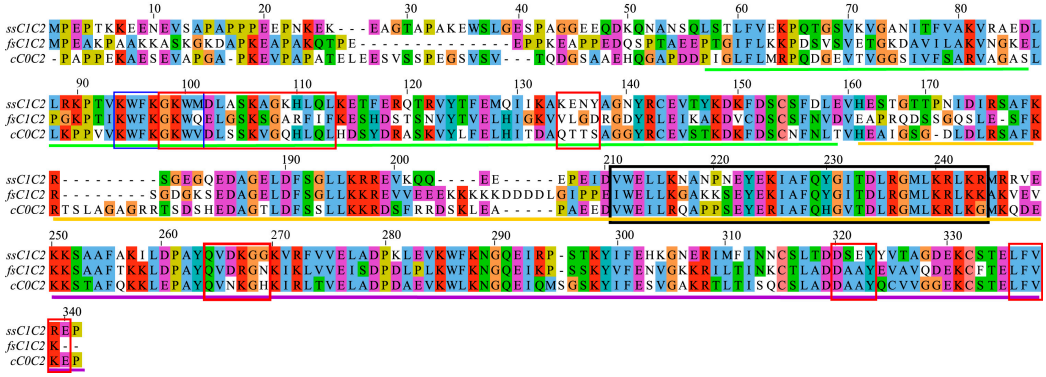

Figure 1. Clustal Omega alignments reveal conservation of amino acid residues in the N-terminal regions containing domains C1-C2 consisting of determinants for myofilament protein interaction in MyBP-C isoforms. The amino acid residues for mouse MyBP-C are aligned using Clustal Omega, demonstrating conservation from Jalview (ClustalX coloring). The corresponding domains are illustrated by a green line (C1), a gold line (M-motif), and a purple line (C2). Known regions of actin binding (red boxes), myosin binding (blue boxes), and overlapping CaM/actin binding sites (black line) for cC0C2 are depicted.

2.2. The Thermal Stability of ssMyBP-C Is Impacted by Ca^{2+}-CaM

Recombinant N-terminal His-tagged ssC1C2 was produced using a T7 expression system and purified with HisTrap columns. CaM was produced and purified as previously described [28]. Following purification, protein samples were visualized by SDS-PAGE and determined to be homogenous. We examined the thermal stability of ssC1C2 in the presence and absence of Ca^{2+}-CaM using DSF experiments. Proteins are subjected to thermal denaturation during DSF, exposing the hydrophobic protein core, which allows for SYPRO Orange dye to interact [33]. Upon binding to hydrophobic environments, the fluorescence of the dye increases relative to the degree of exposed hydrophobic surface area. This permits the protein unfolding to be monitored and the midpoint

of this thermal transition is considered to be the apparent melting temperature (T_m). Changes in T_m occur upon ligand or protein–protein binding, which can increase or decrease the thermal stability of proteins depending on the nature of the binding [33,34], are detected as shift changes in peaks. Given that the N- and C-lobes of CaM have exposed hydrophobic patches, high intrinsic fluorescence was observed for Ca^{2+}-CaM free, which precluded determining its T_m (Figure 2a). To monitor complex formation, MyBP-C proteins were combined with CaM in a final molar ratio of [ssMyBP-C:CaM][1.0:0.5]. The ssC1C2 protein exhibited an apparent T_m 52.4 °C in the absence of CaM, but two T_m measurements of 48.7 °C and 58.0 °C were observed in the presence of Ca^{2+}-CaM (Figure 2; see Figure S1 for derivative data), which suggests that interaction with bilobal CaM may impact the structure in multiple ways. Increased thermal stability upon the addition of Ca^{2+}-CaM is indicative of complex formation. However, the decrease in thermal stability suggests that Ca^{2+}-CaM binding might destabilize a region of ssC1C2.

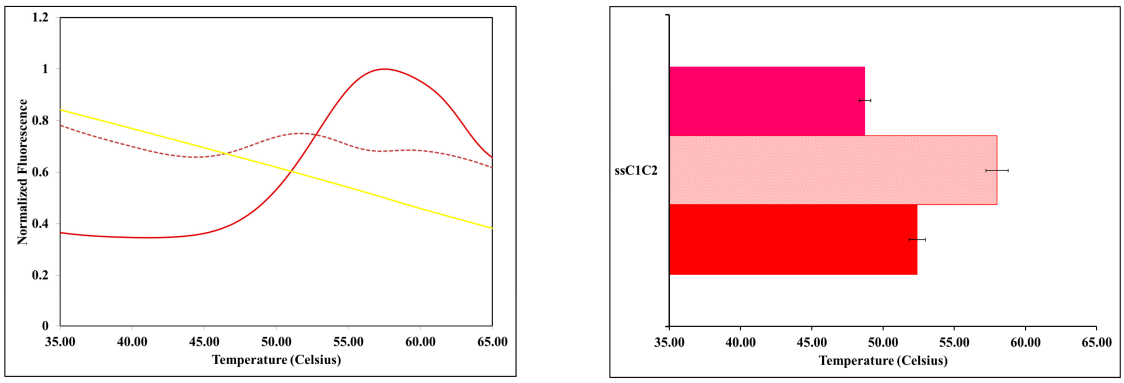

(**a**) (**b**)

Figure 2. Differential scanning fluorimetry experiments show that ssC1C2 has altered thermal stability in the presence of Ca^{2+}-CaM. Normalized fluorescence versus temperature plots are shown for ssC1C2 (red), ssC1C2/CaM (red dash), and free CaM (yellow) (**a**). The T_m determined for ssC1C2 in the presence (hatched and pink bars) and absence (solid red bar) of Ca^{2+}-CaM are shown (**b**).

2.3. CaM-Induced Conformational Modulation of ssC1C2 Is Ca^{2+}-Dependent and Localized Primarily to the M-Motif

NMR binding experiments were performed to monitor conformational changes in [^{15}N]ssC1C2 in the presence of unlabeled Ca^{2+}-CaM. NMR chemical shift values for [^{15}N]ssC1C2 were similar to those reported in the literature [25,30,35–37]. Amide proton nitrogen chemical shift assignments, in particular for indole peaks corresponding to W95, W100, W212, and W286 (W191, W196, W318, and W396 in mouse cMyBP-C), were determined by direct comparison to BMRB accession numbers 6015, 5591, and 17,867. Assessment of 2D ^{1}H-^{15}N spectra for [^{15}N]ssC1C2 free and bound to unlabeled CaM revealed that Ca^{2+}-CaM induced conformational perturbations in numerous peaks (Figure 3a). In particular, M-motif residues V211, W212, E213, K216, N217, A218, Y223, E224, R236, G237, K240, L242, and K243 showed reduced intensities upon the addition of CaM suggesting that Ca^{2+}-CaM interacts with this region. Furthermore, the indole peak for W212, also mapping to the M-motif, experienced significant broadening upon saturation with Ca^{2+}-CaM. After the addition of an excess of CaM, W212 in the M-motif broadened beyond detection while the indole peaks mapping to the C1 (W95 and W100) and C2 (W286) domains did not experience conformational changes. Modest conformational perturbations were detected in residues A253 and A254, suggesting a limited role for the C2 domain in Ca^{2+}-CaM binding. The dissociation constant was determined to be 15–30 μM (data not shown), which is similar to that previously reported [25]. When the binding was repeated in the presence of the Ca^{2+} chelator EDTA (Figure 3b), no detectable conformational changes were observed in ssC1C2, which suggests that Ca^{2+} plays a significant role in mediating this interaction.

Taken together, the NMR binding studies support that the M-motif of ssC1C2 associates with CaM in a Ca^{2+}-dependent manner.

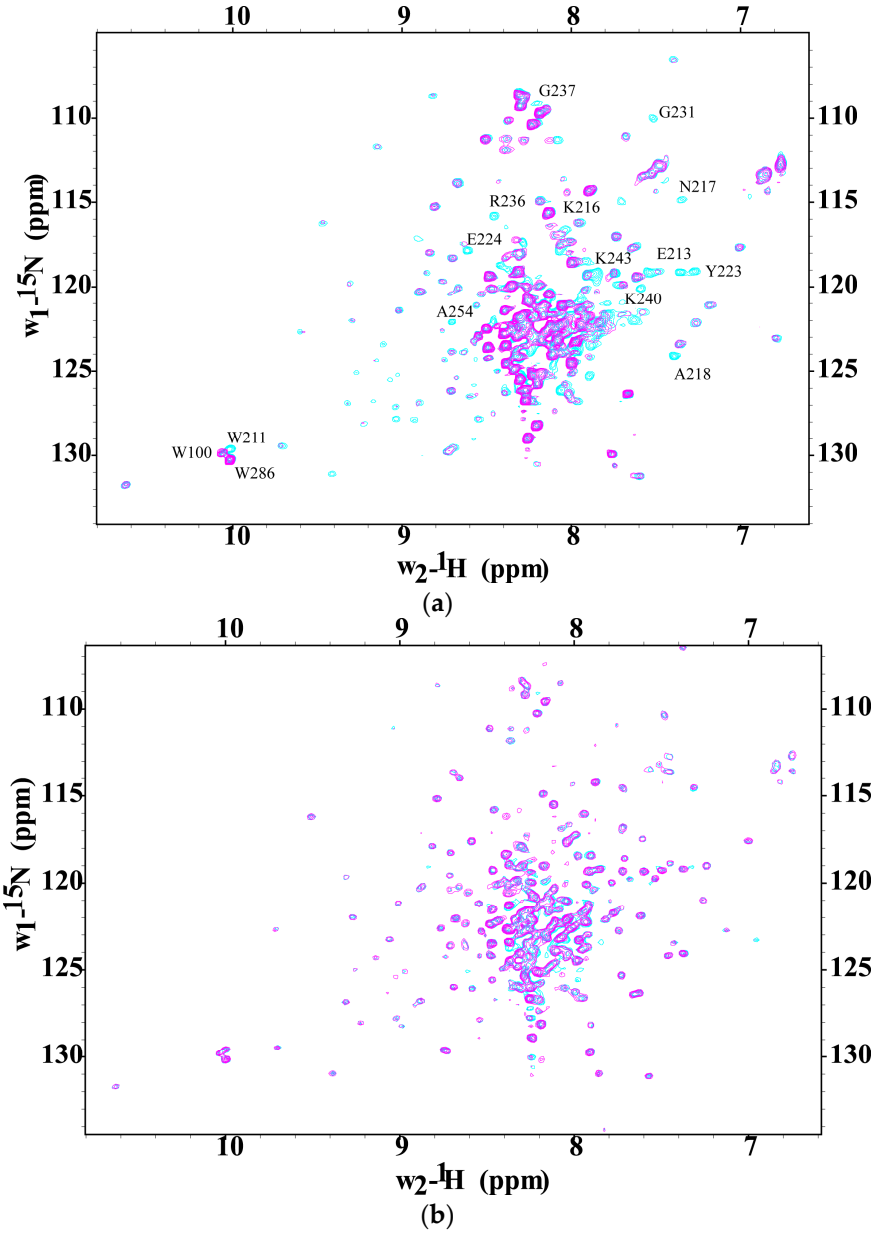

Figure 3. CaM binding is mediated through hydrophobic interaction with primarily the M-motif of ssC1C2. Protein interaction is monitored by comparison of 2D ^{1}H-^{15}N TROSY-HSQC spectra of [^{15}N]ssC1C2 free and bound to unlabeled CaM. Protein interaction is monitored by comparison of 2D ^{1}H-^{15}N TROSY-HSQC spectra of [^{15}N]ssC1C2 free and bound to unlabeled CaM in the presence of 10 mM $CaCl_2$ at 600 MHz. TROSY-HSQC spectra of labeled ssC1C2 (cyan) following the binding with an equimolar amount of Ca^{2+}-loaded CaM (magenta) are superposed (**a**). Multiple resonances mapping to the M-motif and a few mapping to the C2 domain experience conformational perturbation upon the addition of Ca^{2+}-CaM. Select resonances that experience broadening in the presence Ca^{2+}-CaM and the indole resonances for W100, W212, and W286 are labeled. Overlay of spectra of [^{15}N]ssC1C2 free and bound to unlabeled CaM collected in the presence of 5 mM EDTA at 850 MHz. TROSY-HSQC spectra of labeled ssC1C2 (cyan) following the binding with an equimolar amount of CaM (magenta) are superposed in the absence of Ca^{2+}-saturation (**b**). The absence of observable chemical shift perturbations suggests that CaM binding to ssC1C2 is Ca^{2+}-dependent.

The reverse binding experiment was performed where unlabeled ssC1C2 was added to [^{15}N, ^{13}C, ^{2}H]Ca^{2+}-CaM and complex formation was monitored by ^{1}H-^{15}N 2D correlation spectra. Amide proton-nitrogen resonances in [^{15}N, ^{13}C, ^{2}H]Ca^{2+}-CaM shifted or decreased in intensity during ssC1C2 binding. The chemical shift differences were calculated and plotted versus CaM amino acid sequence number (Figure 4a). The following resonances mapping to both the N-terminal and C-terminal domains of CaM experienced significant chemical shift differences in the presence of ssC1C2: S17, L18, F19 D22, D24, V35, I52, D56, D58, M73, Y99, D131, N137, T146. When these residues were colored onto a surface representation of Ca^{2+}-CaM (PDB 1CLL), it is clear that ssC1C2-dependent conformational perturbations are localized to the lobes of CaM (Figure 4b). As predicted, the structural changes occur predominantly in the hydrophobic clefts of CaM, indicating that nonpolar residues, such as methionine, are important in binding ssC1C2. Lu et al. report that cMyBP-C preferentially associates with the C-terminal domain of CaM. More recently, Trewhella and colleagues report that both domains of CaM are involved in interactions with cMyBP-C [38].

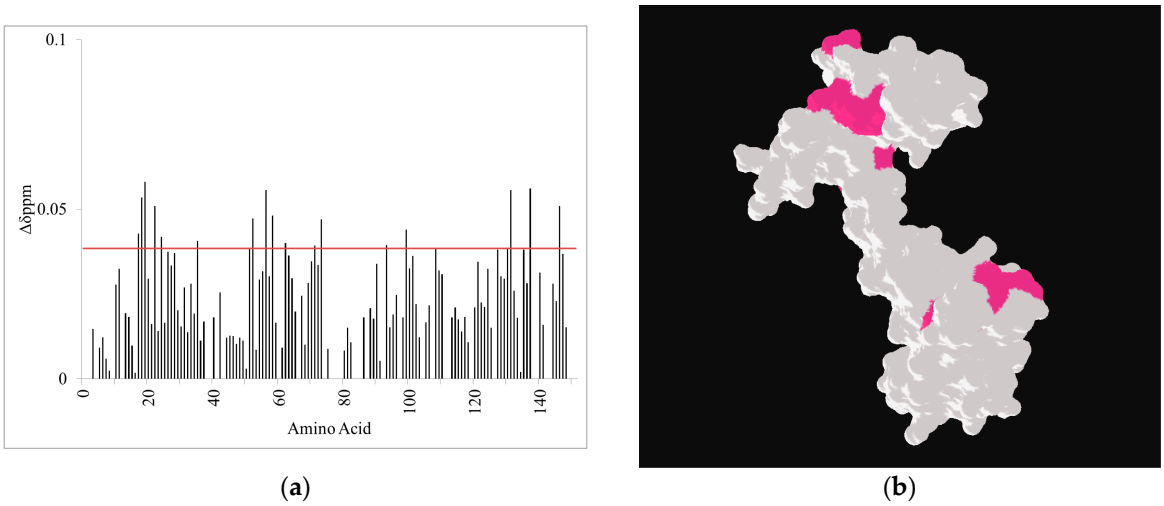

(**a**) (**b**)

Figure 4. The association of ssC1C2 M-motif perturbs both lobes of CaM. Composite amide-proton nitrogen chemical shift differences were calculated between labeled CaM and ssC1C2-bound CaM and plotted versus CaM amino acid residue. The horizontal line is indicative of the average chemical shift difference plus one standard deviation (**a**). The amino acid residues that experience significant chemical shift perturbations in the presence of ssC1C2 are colored pink on the surface representation of Ca^{2+}-loaded CaM (PDB 1CLL) (**b**).

2.4. A Molecular Model Sheds Light on How the M-Motif of MyBP-C Engages Protein Targets

To better understand how the M-motif of ssMyBP-C is folded, we used the SWISS-MODEL to predict 3D structures of this region [39]. The M-motif of mouse cMyBP-C (PDB 2LHU) was used as a template structure. A minimum of 86% sequence coverage was attained and a valid model was chosen based on QMEAN score and PROCHECK analysis [40,41]. Molecular models may be assessed using the QMEAN score, which examines global and local structural qualities. QMEAN scores range from 0 to 1, with a score of 1 being indicative of a high-quality model. The selected ssC1C2 model had a QMEAN score of 0.76, which is considered to be acceptable. In the PROCHECK analysis, the stereochemical quality of a structure was assessed, and we found that the M-motif structure had greater than 90% of residues in the most favored regions, which confirms that the model quality is high. The global fold of M-motif structure for ssC1C2 was similar to the three-helix bundle reported for cMyBP-C (Figure 5a). Both skeletal and cardiac isoforms were comprised of three-helix bundle containing M-motifs and ssC1C2 exhibits similar presentations of exposed charged and nonpolar surface areas (Figure 5b). Furthermore, comparison of M-motif exposed surfaces revealed that positively charged residues such as R236, which have been shown to be involved in CaM and actin binding in cardiac, are

conformationally similar in both isoforms. While the M-motif of ssC1C2 has similarities in accessible hydrophobic surface areas, providing further evidence that this region might engage hydrophobic targets such as Ca^{2+}-CaM in a similar way, a slight difference in polar surfaces is noted (Figure 5b). This reflects the presence of N219 in ssC1C2, which is a P residue in C0C2 cMyBP-C (Figure 1 and Table S2). The P is conserved in the human and mouse cardiac isoform, but varies in the skeletal isoforms.

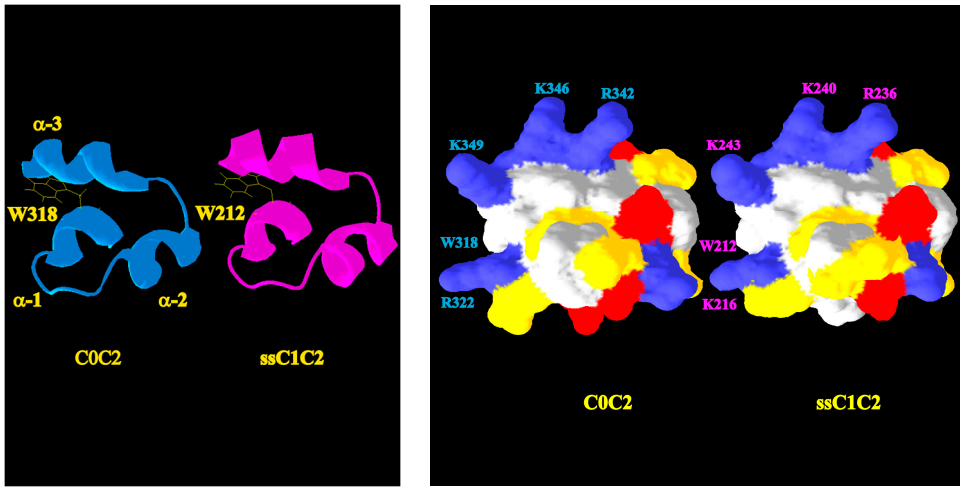

(**a**) (**b**)

Figure 5. Comparison of M-motif structural features in mouse MyBP-Cs. Ribbon structures of the average solution NMR structure of the M-motif from cMyBP-C (PDB 2LHU) (C0C2) (blue) and the molecular model of the M-motif of ssC1C2 (fuchsia) show the triple helix bundle reported to be involved in actin and CaM interactions (**a**). The conserved tryptophan residues from the M-motif of each isoform are indicated in yellow and the helices are numbered from α-helix 1(α-1) through α-helix 3(α-3). Electrostatic surface representations of mouse cardiac and skeletal M-motif structures are shown for C0C2 (PDB 2LHU) and ssC1C2 (molecular model) (**b**). Surfaces are colored according to amino acid type: basic (blue), acidic (red), nonpolar (gray), and polar (yellow). Select amino acid residues W318, R322, R342, K346 for mouse cardiac (blue), which were identified by Lu et al. to be involved in CaM binding to M-motif of cMyBP-C, are labeled. In this study, we found that these key conserved residues labeled W212, K216, R236, K240, and K243 (fuchsia), are also perturbed in ssC1C2 in the presence of Ca^{2+}-CaM.

3. Discussion

In this study, we provide the first known evidence demonstrating that Ca^{2+}-CaM interacts with the M-motif of ssC1C2. We performed DSF and NMR experiments to examine the interaction between ssC1C2 and Ca^{2+}-CaM. We found that ssC1C2 experiences conformational changes in the presence of CaM as evidenced by distinct thermal transitions measured using DSF. Our DSF experiments found that in the presence of Ca^{2+}-CaM, there are both stabilizing and destabilizing binding events occurring, as evidenced by the measurement of two T_m values. These findings might be explained by the differential interactions occurring between ssC1C2 and the N- and C-lobes of Ca^{2+}-CaM. For example, it is possible that association with Ca^{2+}-CaM stabilizes a region of ssC1C2 at or near the M-motif, which would increase the thermal stability. However, binding CaM might promote a structural rearrangement in ssC1C2 that favors unfolding, which would result in reduced thermal stability. Interestingly, Michie and Trewhella report on the modular nature of the M-motif, the C2 domain, and the flexible tether connecting these regions of cMyBP-C [38]. In that same study, they indicate that the tri-helix bundle of the M-motif undergoes changes in helical content, including destabilization of helices in the M-motif, and tertiary organization upon Ca^{2+}-CaM association. However, their data support the idea that stabilizing interactions involving insertion of W318 (W322 in Human cMyBP-C) into the hydrophobic cleft of Ca^{2+}-CaM occur. Our findings in the current study of ssC1C2 are in good agreement with the

observations that Ca^{2+}-CaM binding induces both stabilization and destabilization within the modular regions of N-terminal cMyBP-C. We propose that, in the presence of Ca^{2+}-CaM, these conformational changes result from either direct intermolecular association with ssC1C2 or indirectly through allosteric mechanisms, common regulatory mechanisms by which modular proteins function.

Our NMR binding studies revealed that the M-motif of ssC1C2 engages in site-specific interactions with the hydrophobic lobes of CaM. In the presence of ssC1C2, we found conformational perturbations in the hydrophobic clefts of Ca^{2+}-CaM, indicating its involvement in multi-domain interactions with CaM. We observed conformational perturbation largely localized to the M-motif of ssC1C2 in the presence of CaM, while residues mapping to the C1 and C2 domains remain unchanged. Most notably, we found that W212, which broadens beyond detection in the presence of Ca^{2+}-CaM, is most likely involved in site-specific hydrophobic interactions occurring between these proteins. The Ca^{2+}-CaM-induced exchange broadening of residues mapping to the M-motif of ssC1C2 is likely the consequence of highly dynamic interactions at the binding interface. This exchange broadening phenomenon and conformational fluctuations have been reported in other muscle proteins [42,43]. The NMR observation of conformational plasticity in the M-motif and the C2 linker in ssC1C2 is also consistent with our DSF data showing partial destabilization in the ssC1C2/CaM complex as evidenced by the lowered T_m. Our structural modeling supports that ssC1C2 has an exposed hydrophobic surface area consisting of W212 which would provide a binding surface for Ca^{2+}-CaM. The M-motif W212 is conserved across isoforms and species (Figure 1 and Table S2), which further indicates its importance in MyBP-C structure and function. Moreover, our NMR studies revealed no detectable conformational perturbations in ssC1C2 in the presence of CaM and EDTA, which is in agreement with reports of Ca^{2+}-dependent interaction between CaM and cMyBP-C [25]. This is likely the result of a reduction in hydrophobic surface area in CaM in the presence of EDTA, which disrupts W212 association, further emphasizing the importance of hydrophobic binding in this system. In ssC1C2, the W212R mutation was identified in distal arthrogryposis patients [44]. While the W212R mutant protein localized to the sarcomere, it was predicted to result in dysfunctional regulation of contractility in these patients [44]. Based on our findings, we predict that the M-motif of ssC1C2 may be capable of switching between CaM, actin, and myosin interactions, which would allow it to be an important mediator in interpreting Ca^{2+} signaling in muscle.

Our work provides compelling evidence that ssC1C2 interacts with CaM in a Ca^{2+}-dependent manner. It is possible that interaction with Ca^{2+}-CaM facilitates recruitment of CaMK to this region. Because Ca^{2+}-CaM has a moderate affinity for MyBP-C, it would be possible to rapidly reverse this interaction in the muscle so that Ca^{2+}-CaM may activate CaMK and promote phosphorylation in this region, which may facilitate its dynamic interaction with other muscle regulatory proteins. This finding is significant because it provides justification for pursuing more detailed studies into the role of CaMK and Ca^{2+}-CaM in molecular regulation of skeletal contractility. Previously, CaMK phosphorylation was shown to modulate cMyBP-C conformation, which plays a role in normal contractile function [8]. Lu et al. demonstrated the M-motif of cMyBP-C contains the molecular determinants for Ca^{2+}-CaM binding and its association is not phosphorylation-dependent [25], suggesting that another mechanism must account for CaM's dissociation. However, the conformation of cMyBP-C has been shown to be affected by its phosphorylation state [45], which is directly linked to functional adaption in muscles.

In fact, phosphorylation of myofibrillar proteins is a well-known mechanism for modulating skeletal and cardiac muscle activity, including MyBP-C. In skeletal muscles, CaMK2 activity is affected by cellular [Ca^{2+}], which provides a conduit for fine-tuning Ca^{2+}-responsiveness through Ca^{2+}-CaM-dependent interactions, but the molecular targets are not completely characterized [46]. Phosphorylation-induced modulation of troponin structure in cardiac muscle provides a molecular switch by which the force and frequency of muscle contraction is controlled [47–52]. In previous studies, we have shown that protein kinase A (PKA) phosphorylation of S273, S282, S302, S307 in mouse MyBP-C are critical to the regulation of normal muscle function [8,53]. Phosphorylation of cMyBP-C was demonstrated to modulate its association with actin [54]. A region of importance

in phosphorylation-dependent modulation of motility is the N-terminal region of the M-motif [55]. In addition to PKA, both protein kinase C (PKC) [56] and CaMK2 phosphorylation of cMyBP-C [57] were demonstrated to influence muscle contraction. There is evidence that phosphorylation of the N-terminal region in ssMyBP-C may be critical in skeletal muscle health and disease. In ssMyBP-C, site-specific phosphorylation sites at residues S6 and T84 have been identified as functionally important [26,32], but the role of phosphorylation in fsMyBP-C remains to be determined. Based on the importance of phosphorylation in muscle structure and function, we wanted to look for predicted phosphorylation sites in skeletal MyBP-C, in particular those that might be near the CaM binding site we found in ssC1C2. We used the Group-based Prediction System V3.0 (GPS) software [58] to examine ssC1C2 and fsC1C2 protein sequences for CaMK phosphorylation sites. We found that CaMK phosphorylation sites are predicted at residues S55, T92, T125, T166, S252, S296, S316, and S333 in ssMyBP-C and at positions T81, T110, and S250, and S294 in fsMyBP-C (Table S1). We used GPS to identify known CaMK phosphorylation sites at positions S328, S402, S423, and S440 C0C2. In agreement with other studies, we identified similar CaMK sites that were previously reported in cMyBP-C [53]. These data suggest that functionally relevant CaMK phosphorylation sites are likely to be found in ssMyBP-C and fsMyBP-C. However, more solution structure studies are needed to better understand whether or not phosphorylation of skeletal MyBP-C modulates its target binding.

The current evidence in the field supports that MyBP-C proteins have overlapping structural determinants that modulate target recognition. Even though ssMyBP-C, fsMyBP-C, and cMyBP-C proteins preferentially associate with myofilament proteins in an isoform-dependent manner, these homologous proteins retain the core determinants necessary for myofibrillar association [10,18,59,60]. Conserved amino acid residues in regions mapping to actin and myosin binding sites suggests that MyBP-C proteins share common determinants for interactions with key myofilament proteins (Table S2). Overlapping regions of myosin and actin interaction in N-terminal MyBP-C strongly suggest that it alternates between thin and thick filament binding during the contraction cycle [4]. Dynamic movement between thin and thick filament association would require that MyBP-C's structure be extended in such a way so as to permit it to traverse this conformational space in muscle fibers. Jefferies et al. demonstrated that N-terminal fragments of cMyBP-C, in particular C0C2, are elongated in solution, which would be consistent with the ability to switch between thin and thick interactions. In addition to MyBP-C, other muscle proteins, such as the troponin complex, are known to modulate the force–frequency relationship in muscles by alterations in global conformation propagated through overlapping protein–protein binding motifs. In response to Ca^{2+}-signaling, troponin I alternates between actin and troponin C association, and its interaction with these proteins can be modified by changes cardiac troponin I structure [47,48,52]. Conformational transitions of muscle proteins in response to Ca^{2+}-flux and hormonal stimulation are key regulatory features of fine-tuning muscle performance.

Conformational plasticity has also been reported for MyBP-C. The N-terminal region has been reported to switch between actin and myosin binding, which underscores its regulatory importance in muscles. Hypertrophic mutations in the M-motif (R322Q, E334K, V338D, and L348P in human) are known to impact function and organization of the sarcomere [61]. Corresponding mutations in ssC1C2 (K216Q and E224K) differentially altered sarcomeric localization and regulatory functions of this protein [44]. In a recent report, Michie et al. determined that the C-terminal region of the M-motif and the N-terminal region of the C2 domain are critical in CaM association [38]. In this study we also found that the M-motif is conformationally perturbed in the presence of Ca^{2+}-CaM, with modest changes in residues mapping to the C2 linker region occurring. We found that K216, R236, K240, and K243 in the M-motif and A254 in the C2 linker are perturbed in the presence of Ca^{2+}-CaM. These findings are significant because a number of mutations mapping to M-motif and the region connecting it to C2 in both skeletal and cardiac MyBP-C have been identified as pathogenic in humans, emphasizing that it likely plays a critical role in muscle regulation. Our findings are in agreement with the proposal that this region of MyBP-C is likely involved in dynamic interactions that utilize switching between CaM,

actin, and myosin association as a means by which to modulate contractility. Taken together, these data hint that highly conserved structural determinants are present in skeletal and cardiac isoforms of MyBP-C, which are necessary for maintaining core muscle functions, but structural variations outside of these conserved regions may provide the basis for unique isoform-specific features that participate in controlling structure and function is a tissue-dependent manner.

In summary, we have shown that in solution ssC1C2 has distinct conformation and thermal stability in the presence and absence of Ca^{2+}-CaM. We believe that this is the first report indicating that ssC1C2 interacts with Ca^{2+}-CaM by associating with the M-motif, a finding that is relevant given that this region of cMyBP-C is known to contain the core components necessary for actin, myosin, and CaM interactions. Using NMR binding studies, we show that site-specific interaction occurs between the M-motif of ssC1C2 and Ca^{2+}-CaM in a manner that is similar to cMyBP-C, which suggests that Ca^{2+}-CaM-regulated phosphorylation of MyBP-C may also be relevant in skeletal muscle function. Based on these observations, we propose that a critical link between Ca^{2+}-signaling and phosphorylation-induced modulation of contractility may exist for skeletal isoforms of MyBP-C as well. Other studies demonstrate that PKA and PKC phosphorylation of ssMyBP-C impacts normal and diseased states [26,32], but considerably less is known about the role of CaMK-dependent phosphorylation of MyBP-C in skeletal muscle. Current studies in our lab are focused on determining the structural mechanisms of interaction between N-terminal MyBP-C and muscle associated proteins such as actin, myosin, and CaM and what potential role Ca^{2+} has in modulating these interactions. We are using biophysical and biochemical techniques to examine how unphosphorylated and phosphorylated MyBP-C N-terminal fragments associate with myofibrillar proteins. An improved understanding of the molecular mechanisms by which ssMyBP-C, fsMyBP-C, and cMyBP-C regulate muscle contraction offers the potential to develop novel therapeutic and diagnostic approaches to treat muscle diseases.

4. Materials and Methods

4.1. Recombinant Protein Expression and Purification

The mouse gene encoding for ssC1C2 (domains C1C2 for slow skeletal MyBP-C; Uniprot Q6P6L5) was cloned into the pET-28a$^+$ vector (EMD Millipore, Burlington, MA, USA) and recombinant proteins were overproduced in *Escherichia coli* BL21(DE3) cells (Lucigen, Middleton, WI, USA). Briefly, the transformed cells were inoculated in Luria-Bertani (LB) media with the appropriate antibiotic selection and grown at 37 °C with shaking (250 rpm). When the optical density (OD_{600}) reached 1.0–1.5, recombinant protein expression was induced with the addition of isopropyl-1-thiogalactopyroside (IPTG) and growth was continued for 20 h at 15 °C. Stable isotope enrichment of ssC1C2 was achieved using the protocol described above, except the cells were grown in M9 media supplemented with $^{15}NH_4Cl$ (1.0 g/L) or $^{15}NH_4Cl$ and [$^{13}C_6$]-glucose. Recombinant MyBP-C proteins were extracted from cell pellets by sonication in the presence of a lysis buffer containing 500 mM NaCl, 20 mM imidazole, 20 mM Tris-HCl pH 8.0, 5 mM 2-mercaptoethanol (βME), and 1 mM phenylmethanesulfonylfluoride (PMSF). N-terminal fragments of MyBP-C were resolved using HisTrap^{TM} HP Nickel-Sepharose resin (GE Healthcare, Little Chalfont, UK). The isoforms were eluted from columns with increasing concentrations of imidazole. Recombinant proteins were identified as homogenous as analyzed by sodium dodecyl sulfate polyacrylamide gel electrophoresis (SDS-PAGE). Samples containing MyBP-C were dialyzed against 1X phosphate buffered saline (PBS) supplemented with 1.0 mM tris(2-carboxyethyl)phosphine (TCEP). Protein concentrations were calculated by Bradford assay and UV-absorbance at 280 nm based on molecular extinction coefficients for each recombinant MyBP-C.

Stable isotope-labeled and unlabeled CaM were expressed, purified, and quantified as previously described [28]. ApoCaM was prepared by dialyzing purified recombinant proteins against 4 L of buffer containing 250 mM NaCl, 20 mM EDTA, 20 mM EGTA, 20 mM Hepes pH 7.3, and 1 mM PMSF. Following preparation, the metal bound state of CaM was monitored by ^{1}H-NMR.

4.2. Differential Scanning Fluorimetry (DSF) Experiments

For DSF analyses, stock solutions ssC1C2 and CaM were suspended at 20 μM in 1X PBS supplemented with 1.0 mM TCEP. A master mix was prepared by adding 50 μL of protein (5 μM final concentration), 2 μL of SYPRO® Orange (final concentration was 5×), and the volume was adjusted to 200 μL using buffer solution supplemented with tris(2-carboxyethyl)phosphine and 1 mM $CaCl_2$. For protein complexes, master mix samples consisting of 5 μM of ssC1C2 was combined with 2.5 μM of CaM in the presence of 5× SYPRO orange. All samples of free ssC1C2 and CaM-containing MyBP-C mixtures were incubated for 1 h at room temperature. Allotments of 40 μL were loaded into 96-well 0.2 mL thin-wall PCR plates and sealed with iCycler optical quality sealing tape (BioRad, Hercules, CA, USA). Three independent measurements were collected in triplicate for each reaction on a Bio-Rad, Hercules, CA, USA iCycler iQ Real-Time Detection System. Thermal denaturation experiments were performed from 25 °C to 95 °C (0.5 °C/min using 5 s equilibration intervals) with fluorescence excitation and detection at 490 to 575 nm respectively, with the HEX filter. Fluorescence data were normalized over the temperature range with respect to differences in molar ratios. The midpoint for each MyBP-C thermal transition was calculated by taking the first order derivative of the melt curve for each independent measurement (see Figure S1 for derivative data). The average T_m and standard deviation were calculated for ssC1C2 in the presence and absence of Ca^{2+}-CaM.

4.3. Nuclear Magnetic Resonance Spectroscopy (NMR)

NMR experiments were performed on Bruker Avance (Bruker BioSpin, Billerica, MA, USA) III 600 MHz and 850 MHz spectrometers equipped with conventional 5-mm probes. Two-dimensional (2D) Heteronuclear Single Quantum Coherence (^{1}H-^{15}N-HSQC) or Transverse Relaxation Optimized (^{1}H-^{15}N TROSY-HSQC) spectra were collected for all samples at 298 K. For NMR analyses, a sample consisting of [^{15}N]ssC1C2 or [^{15}N, ^{13}C]ssC1C2 was suspended in NMR buffer composed of 1X PBS buffer supplemented with 1.0 mM TCEP and 10% ^2H_2O at a final concentration of 130 μM–500 μM in the presence of 10 mM $CaCl_2$ or 5 mM EDTA. The backbone chemical shift assignments for stable isotope-labeled ssC1C2 were determined in part by direct comparison to the previously known values (BMRB accession numbers 17,867, 11,212 and 5591). The following suite of triple-resonance experiments were used to confirm assignments: ^{15}N edited NOESY-HSQC, CβCαCONH, HNCA, TROSY-HNCO, and TROSY-HNCA [28]. Samples of [^{15}N, ^{13}C, ^{2}H]Ca^{2+}-CaM were also suspended at 130 μM in NMR buffer in the presence of 10 mM $CaCl_2$. Based on our previous NMR studies [28], the chemical shifts for [^{15}N, ^{13}C, ^{2}H]Ca^{2+}-CaM were readily assigned in the current NMR buffer. NMR data were processed using NMRPipe [62] and analyzed using Sparky [63].

For NMR binding experiments, 2D ^{1}H-^{15}N-HSQC or TROSY-HSQC spectra of free [^{15}N, ^{13}C]ssC1C2 and free [^{15}N, ^{13}C, ^{2}H]Ca^{2+}-CaM were separately collected. NMR binding studies were performed by adding allotments of unlabeled CaM to [^{15}N, ^{13}C]ssC1C2 to a final CaM:ssC1C2 molar equivalent of [1.5:1.0] in the presence of 10 mM $CaCl_2$ or 5 mM EDTA. Following addition, samples were mechanically mixed, incubated at ambient temperature, and 2D ^{1}H-^{15}N correlation spectra were collected. In the reverse experiment, samples consisting of [^{15}N, ^{13}C, ^{2}H]Ca^{2+}-CaM were analyzed for ssC1C2 binding by NMR. The interaction of [^{15}N, ^{13}C, ^{2}H]Ca^{2+}-CaM with unlabeled ssC1C2 was monitored after addition ssC1C2 to a final molar ratio of [^{15}N, ^{13}C, ^{2}H]Ca^{2+}-CaM:ssC1C2] at [1:1]. Changes in NMR spectra were monitored by measuring peak intensities and the calculation of amide-proton nitrogen chemical shift differences, which were determined as described [28].

4.4. Homology Modeling and Bioinformatics

Protein homology models were generated for the M-motif of ssMyBP-C using the SWISS-MODEL Workspace [39]. The amino acid sequences corresponding to the M-motif of ssMyBP-C were used as the target, and mouse template structures (PDB 2LHU) were used for tertiary structure prediction. The quality of each model was estimated based on QMEAN scores [40] followed by PROCHECK

evaluation using the PBDsum server [41]. The amino acid sequences of mouse C0C2, fsC1C2, and ssC1C2 were aligned using CLUSTAL Omega [31]. To examine protein sequences for putative phosphorylation sites, we used the GPS 3.0 software [58].

Supplementary Materials: The following are available online at www.mdpi.com/2312-7481/4/1/1/s1, Table S1. Predicted CaMK phosphorylation sites of MyBP-C N-terminal fragments identified using GPS 3.0 (medium threshold); Table S2. Amino acid sequences show conservation between mouse and human M-motif regions; Figure S1. The derivatives of DSF curves are shown with minima revealing the T_m: (a) ssC1C2; (b) ssC1C2 in the presence of Ca^{2+}-CaM.

Acknowledgments: We gratefully acknowledge the contribution of Andor Kiss in supervising and maintaining the instrumentation in the Center for Bioinformatics and Functional Genomics (CBFG). Also, we would like to express our gratitude to Xiaoyun Deng for her technical assistance in the CBFG. We thank Theresa Ramelot for maintaining the NMR spectrometers. The authors appreciate the helpful discussion and insightful comments provided by Gary Lorigan during the preparation of this manuscript. T.I.S., C.W.J., J.C., and N.L.F. were supported in part by DUOS and CFR grants from Miami University. B.L.L. and S.S. were supported by National Institutes of Health (NIH) grants R01HL130356, R01HL105826, K02HL114749, and American Heart Association, Cardiovascular Genome-Phenome Study 15CVGPSD27020012. N.L.F. was supported in part by N.I.H. grant R15GM117478. N.L.F. and C.W.J. were supported in part by United States Department of Agriculture (USDA) Project number 6034-22000-041-24.

Author Contributions: T.I.S., C.W.J., and J.C. carried out experiments and data analyses. J.C. performed bioinformatics analyses. B.L.L. and S.S. established target regions for gene cloning and carried out sub-cloning for plasmid constructs. N.L.F. conceived study design and performed data analyses. T.I.S. and N.L.F. wrote the manuscript.

Conflicts of Interest: The authors declare no conflict of interest.

References

1. Luther, P.K.; Winkler, H.; Taylor, K.; Zoghbi, M.E.; Craig, R.; Padron, R.; Squire, J.M.; Liu, J. Direct visualization of myosin-binding protein C bridging myosin and actin filaments in intact muscle. *Proc. Natl. Acad. Sci. USA* **2011**, *108*, 11423–11428. [CrossRef] [PubMed]
2. Shaffer, J.F.; Kensler, R.W.; Harris, S.P. The myosin-binding protein C motif binds to F-actin in a phosphorylation-sensitive manner. *J. Biol. Chem.* **2009**, *284*, 12318–12327. [CrossRef] [PubMed]
3. Kensler, R.W.; Shaffer, J.F.; Harris, S.P. Binding of the *N*-terminal fragment C0–C2 of cardiac MyBP-C to cardiac F-actin. *J. Struct. Biol.* **2011**, *174*, 44–51. [CrossRef] [PubMed]
4. Lu, Y.; Kwan, A.H.; Trewhella, J.; Jeffries, C.M. The C0C1 fragment of human cardiac myosin binding protein C has common binding determinants for both actin and myosin. *J. Mol. Biol.* **2011**, *413*, 908–913. [CrossRef] [PubMed]
5. Rybakova, I.N.; Greaser, M.L.; Moss, R.L. Myosin Binding Protein C Interaction with Actin: Characterization and Mapping of the Binding Site. *J. Biol. Chem.* **2011**, *286*, 2008–2016. [CrossRef] [PubMed]
6. Bhuiyan, M.S.; Gulick, J.; Osinska, H.; Gupta, M.; Robbins, J. Determination of the critical residues responsible for cardiac myosin binding protein {C's} interactions. *J. Mol. Cell. Cardiol.* **2012**, *53*, 838–847. [CrossRef] [PubMed]
7. Whitten, A.E.; Jeffries, C.M.; Harris, S.P.; Trewhella, J. Cardiac myosin-binding protein C decorates F-actin: Implications for cardiac function. *Proc. Natl. Acad. Sci. USA* **2008**, *105*, 18360–18365. [CrossRef] [PubMed]
8. Sadayappan, S.; Gulick, J.; Osinska, H.; Barefield, D.; Cuello, F.; Avkiran, M.; Lasko, V.M.; Lorenz, J.N.; Maillet, M.; Martin, J.L.; et al. A critical function for Ser-282 in cardiac myosin binding protein-C phosphorylation and cardiac function. *Circ. Res.* **2011**, *109*, 141–150. [CrossRef] [PubMed]
9. Okagaki, T.; Weber, F.E.; Fischman, D.A.; Vaughan, K.T.; Mikawa, T.; Reinach, F.C. The Major Myosin-Binding Domain of Skeletal Muscle MyBP-C (C-Protein) Resides in the COOH-Terminal, Immunoglobulin-C2 Motif. *J. Cell Biol.* **1993**, *123*, 619–626. [CrossRef] [PubMed]
10. Gruen, M.; Prinz, H.; Gautel, M. cAPK-phosphorylation controls the interaction of the regulatory domain of cardiac myosin binding protein C with myosin-S2 in an on-off fashion. *FEBS Lett.* **1999**, *453*, 254–259. [CrossRef]
11. Ratti, J.; Rostkova, E.; Gautel, M.; Pfuhl, M. Structure and interactions of myosin-binding protein C domain C0: Cardiac-specific regulation of myosin at its neck? *J. Biol. Chem.* **2011**, *286*, 12650–12658. [CrossRef] [PubMed]

12. Freiburg, A.; Gautel, M. A molecular map of the interactions between titin and myosin-binding protein C. Implications for sarcomeric assembly in familial hypertrophic cardiomyopathy. *Eur. J. Biochem.* **1996**, *235*, 317–323. [CrossRef] [PubMed]
13. Miyamoto, C.A.; Fischman, D.A.; Reinach, F.C. The interface between MyBP-C and myosin: Site-directed mutagenesis of the CX myosin-binding domain of MyBP-C. *J. Muscle Res. Cell Motil.* **1999**, *20*, 703–715. [CrossRef] [PubMed]
14. Flashman, E.; Watkins, H.; Redwood, C. Localization of the binding site of the *C*-terminal domain of cardiac myosin-binding protein-C on the myosin rod. *Biochem. J.* **2007**, *401*, 97–102. [CrossRef] [PubMed]
15. Kuster, D.W.D.; Govindan, S.; Springer, T.I.; Martin, J.L.; Finley, N.L.; Sadayappan, S. A hypertrophic cardiomyopathy-associated MYBPC3 mutation common in populations of South Asian descent causes contractile dysfunction. *J. Biol. Chem.* **2015**, *290*, 5855–5867. [CrossRef] [PubMed]
16. Weber, F.E.; Vaughan, K.T.; Reinach, F.C.; Fischman, D.A. Complete sequence of human fast-type and slow-type muscle myosin-binding-protein C (MyBP-C). Differential expression, conserved domain structure and chromosome assignment. *Eur. J. Biochem.* **1993**, *216*, 661–669. [PubMed]
17. Lin, B.; Govindan, S.; Lee, K.; Zhao, P.; Han, R.; Runte, K.E.; Craig, R.; Palmer, B.M.; Sadayappan, S. Cardiac Myosin Binding Protein-C Plays No Regulatory Role in Skeletal Muscle Structure and Function. *PLoS ONE* **2013**, *8*, e69671. [CrossRef] [PubMed]
18. Alyonycheva, T.N.; Mikawa, T.; Reinach, F.C.; Fischman, D.A. Isoform-specific interaction of the myosin-binding proteins (MyBPs) with skeletal and cardiac myosin is a property of the *C*-terminal immunoglobulin domain. *J. Biol. Chem.* **1997**, *272*, 20866–20872. [CrossRef] [PubMed]
19. Idowu, S.M.; Gautel, M.; Perkins, S.J.; Pfuhl, M. Structure, stability and dynamics of the central domain of cardiac myosin binding protein C (MyBP-C): Implications for multidomain assembly and causes for cardiomyopathy. *J. Mol. Biol.* **2003**, *329*, 745–761. [CrossRef]
20. Cecconi, F.; Guardiani, C.; Livi, R. Analyzing pathogenic mutations of C5 domain from cardiac myosin binding protein C through MD simulations. *Eur. Biophys. J.* **2008**, *37*, 683–691. [CrossRef] [PubMed]
21. Shaffer, J.F.; Razumova, M.V.; Tu, A.Y.; Regnier, M.; Harris, S.P. Myosin S2 is not required for effects of myosin binding protein-C on motility. *FEBS Lett.* **2007**, *581*, 1501–1504. [CrossRef] [PubMed]
22. Mun, J.Y.; Kensler, R.W.; Harris, S.P.; Craig, R. The cMyBP-C HCM variant L348P enhances thin filament activation through an increased shift in tropomyosin position. *J. Mol. Cell. Cardiol.* **2016**, *91*, 141–147. [CrossRef] [PubMed]
23. Bezold, K.L.; Shaffer, J.F.; Khosa, J.K.; Hoye, E.R.; Harris, S.P. A gain-of-function mutation in the M-domain of cardiac myosin-binding protein-C increases binding to actin. *J. Biol. Chem.* **2013**, *288*, 21496–21505. [CrossRef] [PubMed]
24. Orlova, A.; Galkin, V.E.; Jeffries, C.M.J.; Egelman, E.H.; Trewhella, J. The *N*-terminal domains of myosin binding protein C can bind polymorphically to F-actin. *J. Mol. Biol.* **2011**, *412*, 379–386. [CrossRef] [PubMed]
25. Lu, Y.; Kwan, A.H.; Jeffries, C.M.; Guss, J.M.; Trewhella, J. The motif of human cardiac myosin-binding protein C is required for its Ca^{2+}-dependent interaction with calmodulin. *J. Biol. Chem.* **2012**, *287*, 31596–31607. [CrossRef] [PubMed]
26. Ackermann, M.A.; Kontrogianni-Konstantopoulos, A. Myosin binding protein-C slow is a novel substrate for protein kinase A (PKA) and C (PKC) in skeletal muscle. *J. Proteome Res.* **2011**, *10*, 4547–4555. [CrossRef] [PubMed]
27. Schumacher, M.A.; Rivard, A.F.; Bachinger, H.P.; Adelman, J.P. Structure of the gating domain of a Ca^{2+}-activated K^+ channel complexed with Ca^{2+}/calmodulin. *Nature* **2001**, *410*, 1120–1124. [CrossRef] [PubMed]
28. Springer, T.I.; Goebel, E.; Hariraju, D.; Finley, N.L. Mutation in the beta-hairpin of the Bordetella pertussis adenylate cyclase toxin modulates N-lobe conformation in calmodulin. *Biochem. Biophys. Res. Commun.* **2014**, *453*, 43–48. [CrossRef] [PubMed]
29. Heller, W.T.; Krueger, J.K.; Trewhella, J. Further insights into calmodulin-myosin light chain kinase interaction from solution scattering and shape restoration. *Biochemistry* **2003**, *42*, 10579–10588. [CrossRef] [PubMed]
30. Howarth, J.W.; Ramisetti, S.; Nolan, K.; Sadayappan, S.; Rosevear, P.R. Structural insight into unique cardiac myosin-binding protein-C motif: A partially folded domain. *J. Biol. Chem.* **2012**, *287*, 8254–8262. [CrossRef] [PubMed]

31. Sievers, F.; Wilm, A.; Dineen, D.; Gibson, T.J.; Karplus, K.; Li, W.; Lopez, R.; McWilliam, H.; Remmert, M.; Soding, J.; et al. Fast, scalable generation of high-quality protein multiple sequence alignments using Clustal Omega. *Mol. Syst. Biol.* **2014**, *7*, 539. [CrossRef] [PubMed]
32. Ackermann, M.A.; Ward, C.W.; Gurnett, C.; Kontrogianni-Konstantopoulos, A. Myosin Binding Protein-C Slow Phosphorylation is Altered in Duchenne Dystrophy and Arthrogryposis Myopathy in Fast-Twitch Skeletal Muscles. *Sci. Rep.* **2015**, *5*, 13235. [CrossRef] [PubMed]
33. Lavinder, J.J.; Hari, S.B.; Sullivan, B.J.; Magliery, T.J. High-Throughput Thermal Scanning: A General, Rapid Dye-Binding Thermal Shift Screen for Protein Engineering. *J. Am. Chem. Soc.* **2009**, *131*, 3794–3795. [CrossRef] [PubMed]
34. Cimmperman, P.; Baranauskienė, L.; Jachimovičiūtė, S.; Jachno, J.; Torresan, J.; Michailovienė, V.; Matulienė, J.; Sereikaitė, J.; Bumelis, V.; Matulis, D. A Quantitative Model of Thermal Stabilization and Destabilization of Proteins by Ligands. *Biophys. J.* **2008**, *95*, 3222–3231. [CrossRef] [PubMed]
35. Jeffries, C.M.; Lu, Y.; Hynson, R.M.G.; Taylor, J.E.; Ballesteros, M.; Kwan, A.H.; Trewhella, J. Human cardiac myosin binding protein C: Structural flexibility within an extended modular architecture. *J. Mol. Biol.* **2011**, *414*, 735–748. [CrossRef] [PubMed]
36. Ababou, A.; Zhou, L.; Gautel, M.; Pfuhl, M. Sequence specific assignment of domain C1 of the N-terminal myosin-binding site of human cardiac myosin binding protein C (MyBP-C). *J. Biomol. NMR* **2004**, *29*, 431–432. [CrossRef] [PubMed]
37. Ababou, A.; Gautel, M.; Pfuhl, M. Dissecting the *N*-terminal myosin binding site of human cardiac myosin-binding protein C: Structure and myosin binding of domain C2. *J. Biol. Chem.* **2007**, *282*, 9204–9215. [CrossRef] [PubMed]
38. Michie, K.A.; Kwan, A.H.; Tung, C.S.; Guss, J.M.; Trewhella, J. A Highly Conserved Yet Flexible Linker Is Part of a Polymorphic Protein-Binding Domain in Myosin-Binding Protein C. *Structure* **2016**, *24*, 2000–2007. [CrossRef] [PubMed]
39. Biasini, M.; Bienert, S.; Waterhouse, A.; Arnold, K.; Studer, G.; Schmidt, T.; Kiefer, F.; Cassarino, T.G.; Bertoni, M.; Bordoli, L.; et al. SWISS-MODEL: Modelling protein tertiary and quaternary structure using evolutionary information. *Nucleic Acids Res.* **2014**, *42*, W252–W258. [CrossRef] [PubMed]
40. Benkert, P.; Tosatto, S.C.E.; Schomburg, D. QMEAN: A comprehensive scoring function for model quality assessment. *Proteins Struct. Funct. Bioinform.* **2008**, *71*, 261–277. [CrossRef] [PubMed]
41. De Beer, T.A.P.; Berka, K.; Thornton, J.M.; Laskowski, R.A. PDBsum additions. *Nucleic Acids Res.* **2014**, *42*, D292–D296. [CrossRef] [PubMed]
42. Gasmi-Seabrook, G.M.; Howarth, J.W.; Finley, N.; Abusamhadneh, E.; Gaponenko, V.; Brito, R.M.; Solaro, R.J.; Rosevear, P.R. Solution structures of the *C*-terminal domain of cardiac troponin C free and bound to the *N*-terminal domain of cardiac troponin I. *Biochemistry* **1999**, *38*, 8313–8322. [CrossRef] [PubMed]
43. Hoffman, R.M.B.; Blumenschein, T.M.A.; Sykes, B.D. An interplay between protein disorder and structure confers the Ca^{2+} regulation of striated muscle. *J. Mol. Biol.* **2006**, *361*, 625–633. [CrossRef] [PubMed]
44. Gurnett, C.A.; Desruisseau, D.M.; McCall, K.; Choi, R.; Meyer, Z.I.; Talerico, M.; Miller, S.E.; Ju, J.S.; Pestronk, A.; Connolly, A.M.; et al. Myosin binding protein C1: A novel gene for autosomal dominant distal arthrogryposis type 1. *Hum. Mol. Genet.* **2010**, *19*, 1165–1173. [CrossRef] [PubMed]
45. Michalek, A.J.; Howarth, J.W.; Gulick, J.; Previs, M.J.; Robbins, J.; Rosevear, P.R.; Warshaw, D.M. Phosphorylation modulates the mechanical stability of the cardiac myosin-binding protein C motif. *Biophys. J.* **2013**, *104*, 442–452. [CrossRef] [PubMed]
46. Tavi, P.; Westerblad, H. The role of in vivo Ca^{2+} signals acting on Ca^{2+}-calmodulin-dependent proteins for skeletal muscle plasticity. *J. Physiol.* **2011**, *589*, 5021–5031. [CrossRef] [PubMed]
47. Abbott, M.B.; Dong, W.J.; Dvoretsky, A.; DaGue, B.; Caprioli, R.M.; Cheung, H.C.; Rosevear, P.R. Modulation of cardiac troponin c-cardiac troponin I regulatory interactions by the amino-terminus of cardiac troponin I. *Biochemistry* **2001**, *40*, 5992–6001. [CrossRef] [PubMed]
48. Finley, N.; Dvoretsky, A.; Rosevear, P.R. Magnesium—Calcium Exchange in Cardiac Troponin C Bound to Cardiac Troponin I. *J. Mol. Cell. Cardiol.* **2000**, *1446*, 1439–1446. [CrossRef] [PubMed]
49. Dong, W.J.; Chandra, M.; Xing, J.; She, M.; Solaro, R.J.; Cheung, H.C. Phosphorylation-induced distance change in a cardiac muscle troponin I mutant. *Biochemistry* **1997**, *36*, 6754–6761. [CrossRef] [PubMed]

50. Sakthivel, S.; Finley, N.L.; Rosevear, P.R.; Lorenz, J.N.; Gulick, J.; Kim, S.; VanBuren, P.; Martin, L.A.; Robbins, J. In Vivo and in Vitro Analysis of Cardiac Troponin I Phosphorylation. *J. Biol. Chem.* **2005**, *280*, 703–714. [CrossRef] [PubMed]
51. Baryshnikova, O.K.; Li, M.X.; Sykes, B.D. Modulation of cardiac troponin C function by the cardiac-specific *N*-terminus of troponin I: Influence of PKA phosphorylation and involvement in cardiomyopathies. *J. Mol. Biol.* **2008**, *375*, 735–751. [CrossRef] [PubMed]
52. Finley, N.; Abbott, M.B.; Abusamhadneh, E.; Gaponenko, V.; Dong, W.; Gasmi-Seabrook, G.; Howarth, J.W.; Rance, M.; Solaro, R.J.; Cheung, H.C.; et al. NMR analysis of cardiac troponin C-troponin I complexes: Effects of phosphorylation. *FEBS Lett.* **1999**, *453*, 107–112. [CrossRef]
53. Sadayappan, S.; Osinska, H.; Klevitsky, R.; Lorenz, J.N.; Sargent, M.; Molkentin, J.D.; Seidman, C.E.; Seidman, J.G.; Robbins, J. Cardiac myosin binding protein C phosphorylation is cardioprotective. *Proc. Natl. Acad. Sci. USA* **2006**, *103*, 16918–16923. [CrossRef] [PubMed]
54. Colson, B.A.; Rybakova, I.N.; Prochniewicz, E.; Moss, R.L.; Thomas, D.D. Cardiac myosin binding protein-C restricts intrafilament torsional dynamics of actin in a phosphorylation-dependent manner. *Proc. Natl. Acad. Sci. USA* **2012**, *109*, 20437–20442. [CrossRef] [PubMed]
55. Weith, A.; Sadayappan, S.; Gulick, J.; Previs, M.J.; VanBuren, P.; Robbins, J.; Warshaw, D.M. Unique single molecule binding of cardiac myosin binding protein-C to actin and phosphorylation-dependent inhibition of actomyosin motility requires 17 amino acids of the motif domain. *J. Mol. Cell. Cardiol.* **2012**, *52*, 219–227. [CrossRef] [PubMed]
56. Kooij, V.; Boontje, N.; Zaremba, R.; Jaquet, K.; dos Remedios, C.; Stienen, G.J.M.; van der Velden, J. Protein kinase C alpha and epsilon phosphorylation of troponin and myosin binding protein C reduce Ca^{2+} sensitivity in human myocardium. *Basic Res. Cardiol.* **2010**, *105*, 289–300. [CrossRef] [PubMed]
57. Tong, C.W.; Gaffin, R.D.; Zawieja, D.C.; Muthuchamy, M. Roles of phosphorylation of myosin binding protein-C and troponin I in mouse cardiac muscle twitch dynamics. *J. Physiol.* **2004**, *558*, 927–941. [CrossRef] [PubMed]
58. Xue, Y.; Liu, Z.; Cao, J.; Ma, Q.; Gao, X.; Wang, Q.; Jin, C.; Zhou, Y.; Wen, L.; Ren, J. GPS 2.1: Enhanced prediction of kinase-specific phosphorylation sites with an algorithm of motif length selection. *Protein Eng. Des. Sel.* **2011**, *24*, 255–260. [CrossRef] [PubMed]
59. Offer, G.; Moos, C.; Starr, R. A new protein of the thick filaments of vertebrate skeletal myofibrils. *J. Mol. Biol.* **1973**, *74*, 653–676. [CrossRef]
60. Squire, J.M.; Luther, P.K.; Knupp, C. Structural evidence for the interaction of C-protein (MyBP-C) with actin and sequence identification of a possible actin-binding domain. *J. Mol. Biol.* **2003**, *331*, 713–724. [CrossRef]
61. Harris, S.P.; Lyons, R.G.; Bezold, K.L. In the thick of it: HCM-causing mutations in myosin binding proteins of the thick filament. *Circ. Res.* **2011**, *108*, 751–764. [CrossRef] [PubMed]
62. Delaglio, F.; Grzesiek, S.; Vuister, G.W.; Zhu, G.; Pfeifer, J.; Bax, A. NMRPipe: A multidimensional spectral processing system based on UNIX pipes. *J. Biomol. NMR* **1995**, *6*, 277–293. [CrossRef] [PubMed]
63. Goddard, T.D.; Kneller, D.G. Sparky—NMR Assignment and Integration Software. Available online: https://www.cgl.ucsf.edu/home/sparky/ (accessed on 16 December 2017).

© 2017 by the authors. Licensee MDPI, Basel, Switzerland. This article is an open access article distributed under the terms and conditions of the Creative Commons Attribution (CC BY) license (http://creativecommons.org/licenses/by/4.0/).